(NASA-CR-146430) STUDIES IN SUPPORT OF THE ANALYSIS OF ASTRONOMICAL DATA FROM APOLLO 16 Final Technical Report, 1 Dec. 1974 - 31 Aug. 1975 (Cornell Univ.) 33 p HC $4.00 CSCL 03A G3/89

N76-19019

Unclas 20596

CORNELL UNIVERSITY

Center for Radiophysics and Space Research

ITHACA, N. Y.

CRSR 628

STUDIES IN SUPPORT OF THE ANALYSIS OF

ASTRONOMICAL DATA FROM APOLLO 16

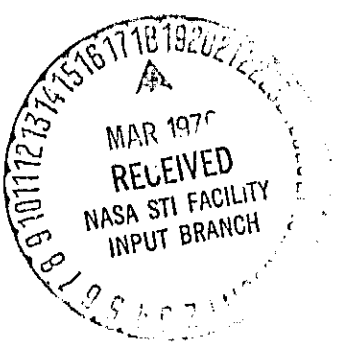

Final Technical Report

NASA RESEARCH GRANT NSG 5037
December 1, 1974 - August 31, 1975

Principal Investigator: Prof. K. I. Greisen

March 1976

STUDIES IN SUPPORT OF THE ANALYSIS OF ASTRONOMICAL DATA FROM APOLLO 16

Final Technical Report

Professor K. I. Greisen, Principal Investigator
Cornell University
Ithaca, New York 14853

NASA Research Grant NSG 5037

December 1, 1974 to August 31, 1975

SUMMARY

The Apollo Gamma Ray Spectrometer which was part of the scientific instrument module aboard Apollo 16 obtained more than 20 hours of astronomical data near the end of the transearth coast phase of the mission. During this time the vehicle was maneuvered so that every part of the sky as seen by the spectrometer was eventually occulted by the space-craft, providing a valuable data base for gamma ray astronomy in th 30 keV to 5 MeV spectral range.

Much information is available but full analysis has awaited funding. This report discusses analysis schemes classified according to the underlying assumed source distribution. It is known that there is at least one point source, the Crab, and it can be seen in the data. In addition one may expect a distribution around the Galactic plane such as Uhuru found in the 1-10 keV energy region, and one may expect a distribution of diffuse gamma-radiation outside the galactic plane.

The sensitivity function of the space-craft-spectrometer occultation telescope has not been determined yet. The pattern of count rate as a function of the position of the Crab suggests that the occultation pattern is 110° wide (as if the spectrometer were only 0.46 m (1.5 ft) from the space-craft). while the nominal pattern is 62° wide (assuming the spectrometer were the nominal 1.84 m (6 ft) away from the vehicle).

Methods for data analysis are shown in section III. In one method looking only for point sources, some pre-

liminary results concerning the Crab nebula are presented which confirm previous measurement of the strength of that source.

I. Introduction

A. The Apollo Gamma Ray Spectrometer

For the Apollo J-Series missions, Apollo 15 and Apollo 16, a Scientific Instrument Module (SIM) was prepared and installed in the Service Module (SM) to take advantage of the lunar orbit platform available for lunar research during Apollo missions. The J-Series SIM included a gamma-ray spectrometer to study lunar surface composition by measurements of nuclear radioactivity, both natural in origin and induced by cosmic rays.

The Apollo Gamma Ray Spectrometer (AGRS) consisted of a detector, anticoincidence mantle, electronics, and a thermal shield mounted on an extendable boom. The detector was a 7cm x 7cm cylinder of thallium activated sodium iodide [Na(Tℓ)] viewed by a 7.6cm photomultiplier tube while the anti-coincidence mantle, a 0.8 cm thick plastic scintillator covering all sides but one face of the detector, provided an efficient veto pulse for cosmic rays penetrating the detector. The electronics were located toward the space-craft from the detector, and the entire assembly was encased in a thermal shield which added approximately 50 kg m^{-2} (5g cm^{-2}) between the anti-coincidence mantle and space (Harryington, et al., 1974). The boom could be extended to a distance of 7.68 m(25 ft.) from the space-craft to reduce background and was fully deployed for most of the lunar orbit phase of the mission.

The nominal energy range of the instrument was 60 keV

to about 7 MeV, although gain drifts in both missions changed these limits somewhat. During Apollo 15, for instance, spectra were acquired up to 30 MeV. The gain drift was quite a bit less for Apollo 16. Energy loss spectra consisted of 512 linearly spaced channels of accumulated pulse-heights. Instrument live-time was accumulated, transmitted, and reset once every 0.328 s as were the number of shield counts and the number of coincidence counts accumulated in that data frame. Except during the transmission of these data and the frame sync code, the telemetry sampled the output register for a pulse-height once every 2.56 ms.

Principal investigator for the AGRS is Dr. James R. Arnold of UCSD. Co-investigators are Drs. Albert Metzger of JPL, J. I. Trombka of GSFC, and L. E. Peterson of UCSD. It was with their help that the present work was done.

B. AGRS Astronomy

For lunar surface studies the cosmic gamma-ray sources comprise a background which can be neglected in the first approximation but which is worrisome enough to deserve investigation. For gamma-ray astronomy, though, the Apollo J-Series missions provided a unique opportunity to fly a large detector with good spectral resolution sensitive to a relatively unexplored region of the spectrum. Two advantages of being part of a manned vehicle were the virtually unlimited telemetry capacity and a chance to observe far from the earth and its trapped radiation belt. For astronomical

purposes the lunar contribution is background, and one does better astronomy far from the moon. Most of the astronomical results will come from anal the Trans Earth Coast (TEC) data.

Three results in low energy gamma-ray astronomy based on the AGRS data have already been published. The first is a measurement of the spectrum of cosmic gamma rays deduced by Trombka et al. (1973). The second is part of the Apollo 16 Preliminary Science Report (Arnold, et al., 1972) showing the effects of space-craft occultation of the Crab and Galactic Center in the detector count rates. The third published result is a report of the gamma-ray transient source of 27 April, 1972, first discovered in the AGRS data; see Metzger, et al. (1974) and Trombka, Schmadebeck, et al. (1974). Other possibilities include a search for gamma-ray micro-brusts, a search for periodic X-ray sources including the Crab pulsar, and a sky survey using the occultation astronomy data.

Occultation astronomy is an especially challenging and interesting part of the AGRS astronomy potential. Usually in astronomy an instrument is sensitive to a sufficiently small portion of the sky that it can be treated as a flat area, using rectangular coordinates. The analysis of the occultation data will depend on the roundness of the sky in an essential way, and hence require spherical coordinates. Furthermore, there is no axis about which the sensitivity function is symmetric. This means that the

combination of regions occulted is not simply determined by where the detector was pointed; rather, all three dimensions of attitude are needed to determine the exposure of the detector to the sky. There has been discussion of mapping the gamma ray sky in just such a way, using a detector which is sensitive to nearly all of the sky and taking advantage of its anisotropic response to separate components in the sky (Trombka, Vette, et al., 1974). Apollo 16 offers a good data set for a try at this approach, and much will be learned in doing the occultation astronomy.

C. Occultation Astronomy Data Base

During the Apollo 16 mission an effort was made to supply a data base for occultation astronomy. For the last 33 hours of the mission the AGRS was only partially deployed on its boom, nominally at a distance of 1.84 m (6 ft) from the vehicle. Four Passive Thermal Control (PTC) rolling modes were performed in the hope of occulting every part of the sky in at least one of these maneuvers. In addition, a series of pointing modes, with the space-craft in fixed attitudes, were executed as required by other experiments in the SIM. Altogether about 20 hours of live-time were acquired with the AGRS at a fixed distance from the space-craft.

The four PTC modes form the primary data set. The modes and their spin axes were

1. Ecliptic PTC (EPTC), +x at A = 6.0^h, D = -66^{o*}

*A is right ascension, D is declination. See the Appendix on Coordinate Systems, Section VII.

2. Super Galactic Auxill'ary PTC (SGAPTC),

   +x at A = 6.8^h, D = $+15^o$

3. Ecliptic Auxilliary PTC (EAPTC),

   +x at A = 9.4^h, D = $+\cdot 1^o$

4. Super Galactic PTC (SGPTC), +x at A = 18.6^h, D = $+15^o$

SGPTC has approximately 8 hours of live-time, EPTC has 4, EAPTC and SGAPTC have 2 hours each. The counting rates between 0.072 and 0.200 MeV as a function of roll angle for each PTC mode are presented in figures 1-4. The error bars are typical 1σ values. The radial scale is labelled in counts per second. Note that the center of the figure represents 73 cps not zero.

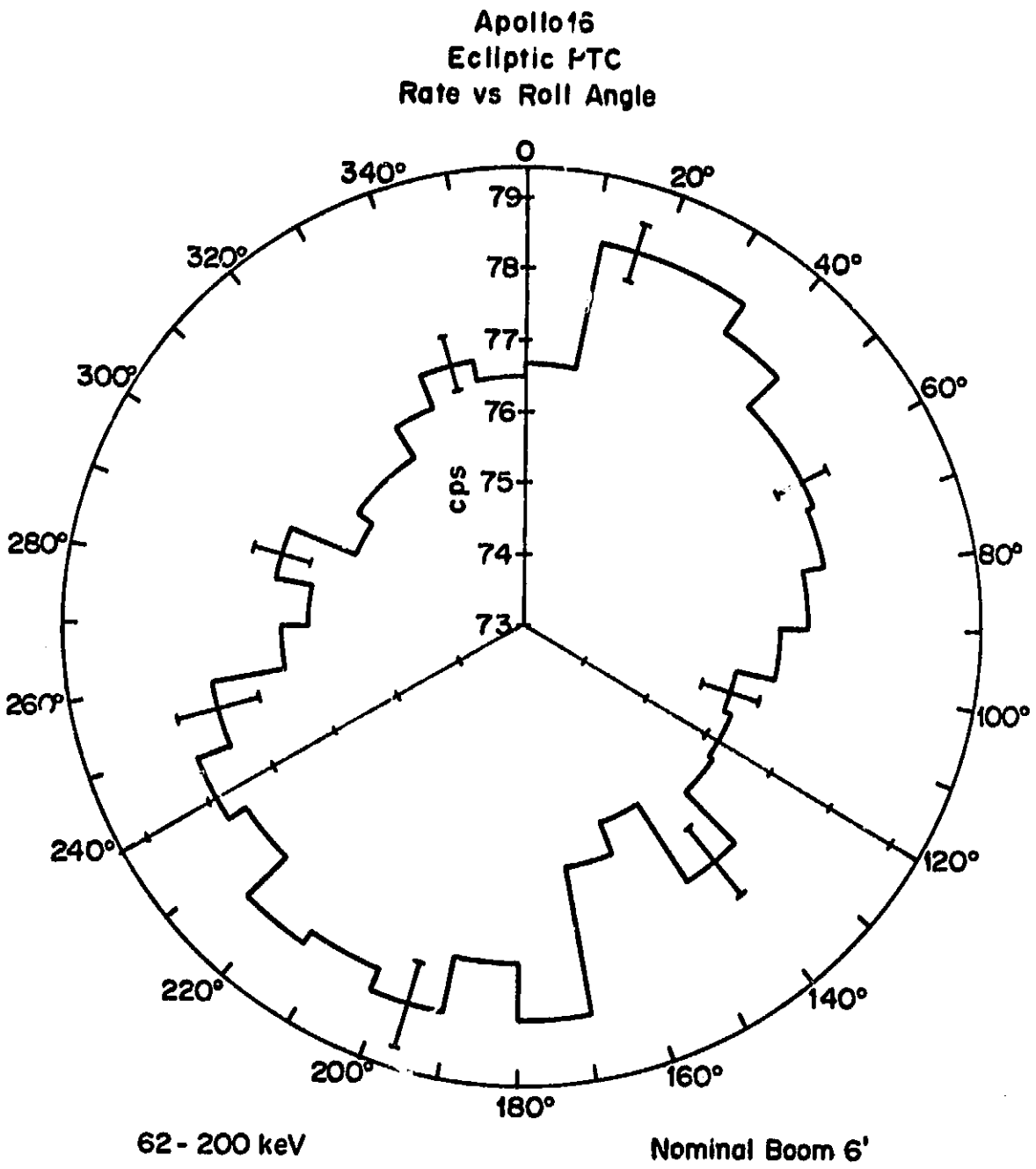

Fig. 1. Rate vs. Roll Angle, Ecliptic PTC.
Rate at center is 73 cps.

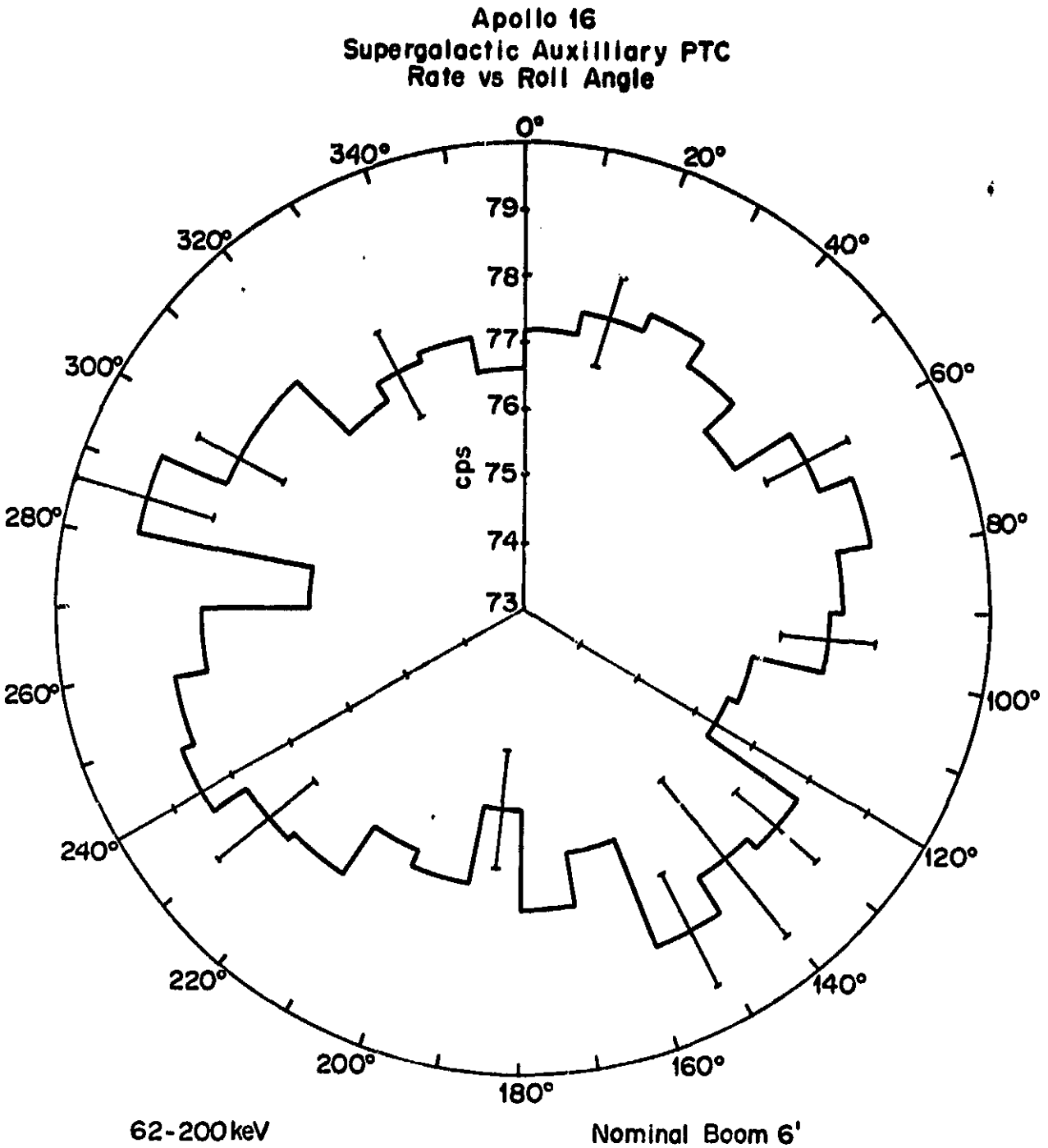

Fig. 2. Rate vs. Roll Angle, Super Galactic Auxilliary PTC. Rate at center is 73 cps.

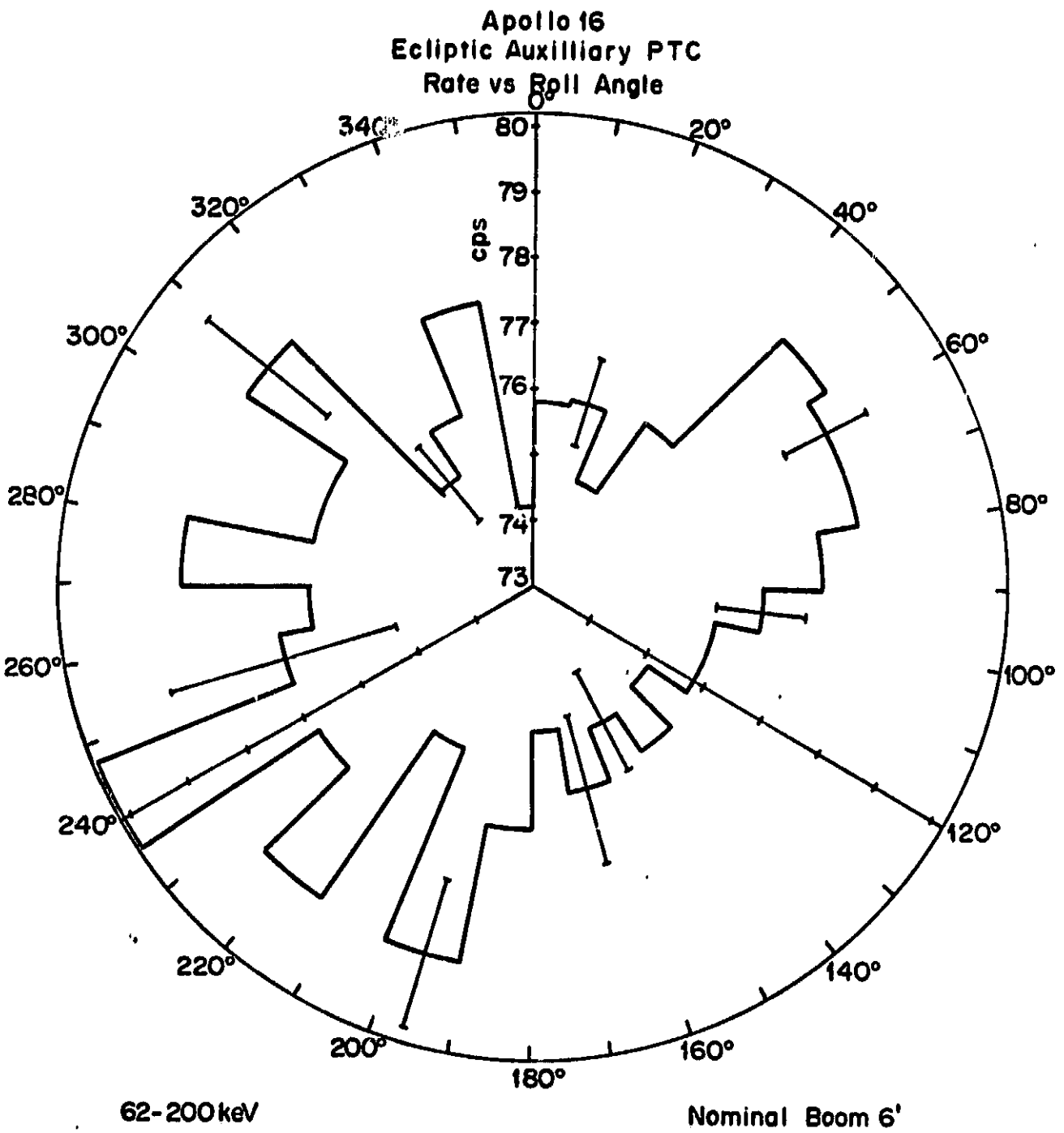

Fig. 3. Rate vs. Roll Angle, Ecliptic Auxilliary PTC. Rate at center is 73 cps.

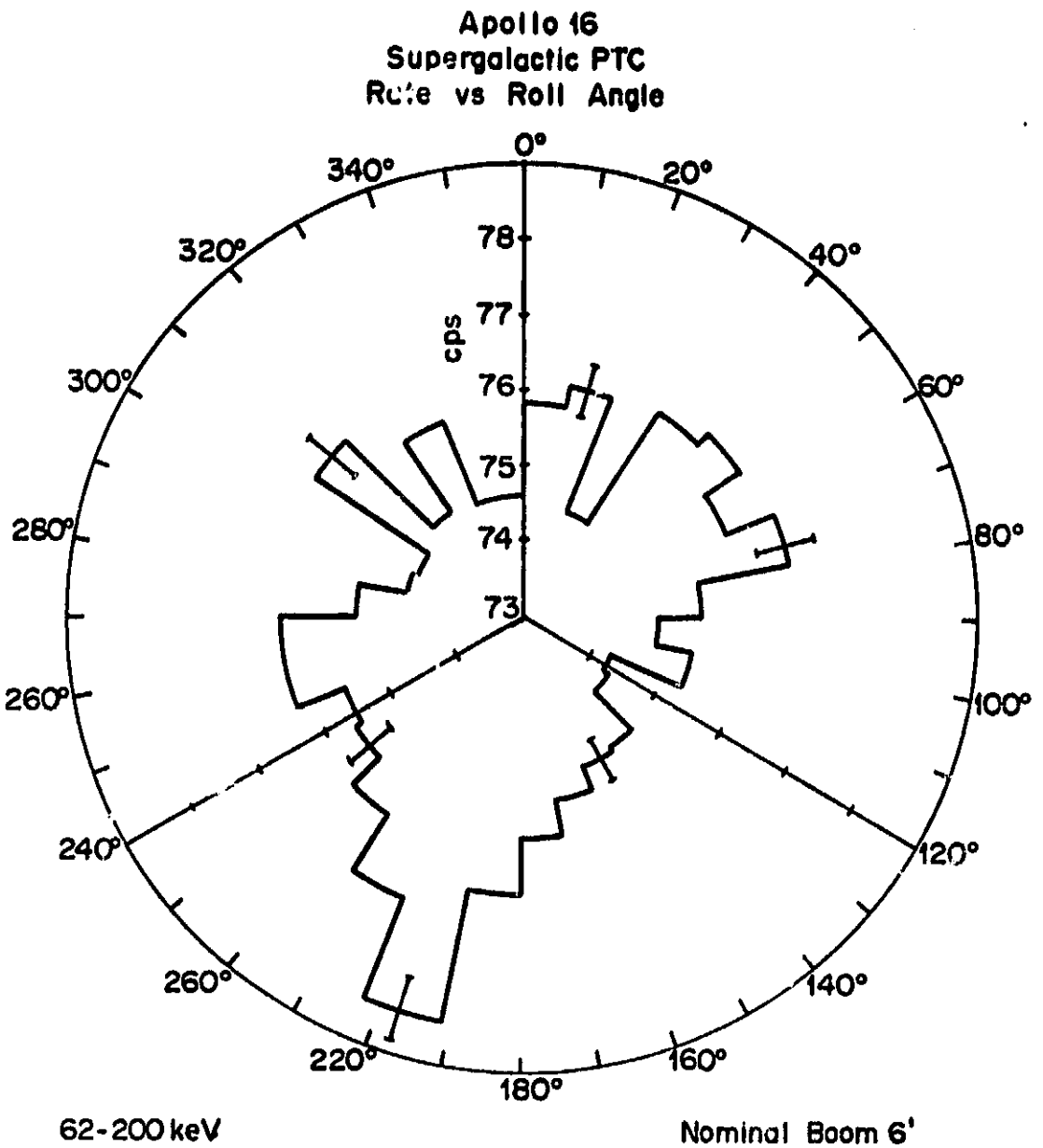

Fig. 4. Rate vs. Roll Angle, Super Galactic PTC. Rate at center is 73 cps.

II. Forms of the Gamma Ray Brightness Distribution

A. Components

There are four source components that are likely to contribute to the counting rate in the detector, an invariant background, a set of a few bright point sources, a line source distributed in the Galactic plane, and an anisotropic diffuse component. The invariant background is made up of contributions from the space-craft, intrinsic detector background induced by cosmic rays, and an isotropic cosmic gamma-ray background. It dominates all the other components.

The bright sources can be expected to include the Crab nebula, which is likely to be responsible for 3% of the flux when it is not occulted, Cygnus X-1, M87 of the Virgo cluster of galaxies, and the Galactic center.

The results of SAS-II at energies above 50 MeV show the Galactic plane to be the dominant source of gamma rays, but in the X-ray range ($<<$ 1 MeV) the dominant source seems to be the diffuse extragalactic component. It may be that the strength of the so-called line source in the Galactic plane will begin to be a major component of the source distribution by 0.5 MeV. It is known that the Galactic center source region at MeV energies is extended rather than point-like.

Finally, there may be an anisotropic diffuse component from extragalactic space, due perhaps to an asymmetry in the local super cluster or the Compton-Getting effect whereby

a Doppler shift gives the isotropic cosmic component a small cos θ dependence about the velocity vector. The isotropy of the diffuse component can have important cosmological implications; see, for instance, Wolfe, 1970.

B. Forms of the Gamma Ray Brightness Distributions

These four components combine in several possible ways depending on their relative strengths, but in any case there will be the invariant background and there will be the Crab nebula. The possible distributions to be considered are

1. A few point sources + invariant background,
2. A few point sources + a line source + invariant background,
3. A few point source + anisotropic diffuse component + invariant background,
4. A few point source + a line source + anisotropic diffuse source + invariant background.

III. The Sensitivty Function

A. Occultation Pattern and Boom Position

Depending on the distance between the detector and the space-craft, the occultation pattern will vary from a solid angle of 0.234 steradians to a few percent more than 2π steradians. Until the boom is extended past 2.76 m (9 ft) the Command Module (CM) is visible only through the SM, and assuming the SM is optically thick, the occultation pattern will be that of a cylinder 3.94 m (154 in) in diameter, extending 3.83 m (149.6 in) above the AGRS boom anchor point and 0.69 m (27.1 in) below it. The assumption of a large optical depth through the SM is valid at low energies (~ 150 keV) but may not be so good abcve 0.5 MeV. The mean density of the SM is $1.3 \cdot 10^{2}$ kg m^{-3} (0.13g cm^{-3}), but the mass is known to be distributed in a clumpy way.

The boom length is known in principle by timing how long the command pilot held the boom extend switch closed. Limit switches closed to indicate fully extended or inboard positions, but intermediate extensions were reckoned from a stopwatch. Unfortunately, the position taken for the occultation astronomy followed a sequence of timed extensions and retractions without knowing any of these intermediate positions with precision. It is also known that the boom deploy mechanism failed at some point because it was not possible to bring the AGRS inboard at the close of the mission.

A recount of the time spent in the assorted extend and retract commands preceding the occultation astronomy position indicates a nominal position of 1.23 m (4 ft) rather than the 1.84 m (6 ft) position the flight directors thought they had. Other indirect methods for determining the boom length have been tried, including studying the flux of charged particles measured as coincidence events between the shield and the detector which varied from 330 coincidences per data frame fully retracted to 265 coincidences per data from fully deployed. The coincidence rate seen at the occultation astronomy position was consistent with an extension of 0.61 m (2 ft). Also, the shield rates were consistent with the rates seen when the AGRS was stowed. These indicate that the detector was very close to the space-craft, but they have a fundamental flaw in the credibility; the shield PMT was known to be noisy before the start of the mission.

Another indirect method is to compare the gamma-ray fluxes in a fixed energy interval of two known extensions with the flux at the occultation astronomy position. Using the fully inboard and the fully deployed fluxes and assuming that the flux due to the space-craft is proportional to the solid angle, a boom position of 1.84 m ± 0.30 m (6 ft ± 1 ft) has been determined, which is consistent with the timing data if one grants that the retraction mechanism failed while the boom was being retracted from 2.46 m (8 ft).

These various results are ambiguous, and in light of the work done here at Cornell on the subject (Section III.D.),

one cannot say that the boom position has been reliably determined. The outline of the space-craft in look-angle coordinates is given in Fig. 5 for a few boom positions.

B. The Effect of Mass Located Around the Detector

A significant amount of mass surrounds the detector itself and it is far from isotropically distributed. One contribution comes from the thermal shield which is more or less isotropic, contributing about 50 kg m^{-2} (5 g cm^{-2}) of absorbing material. However, there is more than 250 kg m^{-2} (25g cm^{-2}) of electronics and supporting structure obscuring the view in back towards the space-craft.

R. H. Parker of JPL computed the column density of absorbing material, seen from the center of the detector volume, in a circle through the top of the detector system. His results are reproduced in Figure 6. 180^{o} is the direction toward the spacecraft while 270^{o} is the direction of the top of the AGRS. The absorber in the direction 270^{o} is the shield PMT.

It is significant that local mass is not likely to be responsible for an occultation pattern much wider than $\pm 25^{o}$ in the direction of the space-craft. Direct measurement with the detector prototype and a Co^{57} source have confirmed this conclusion.

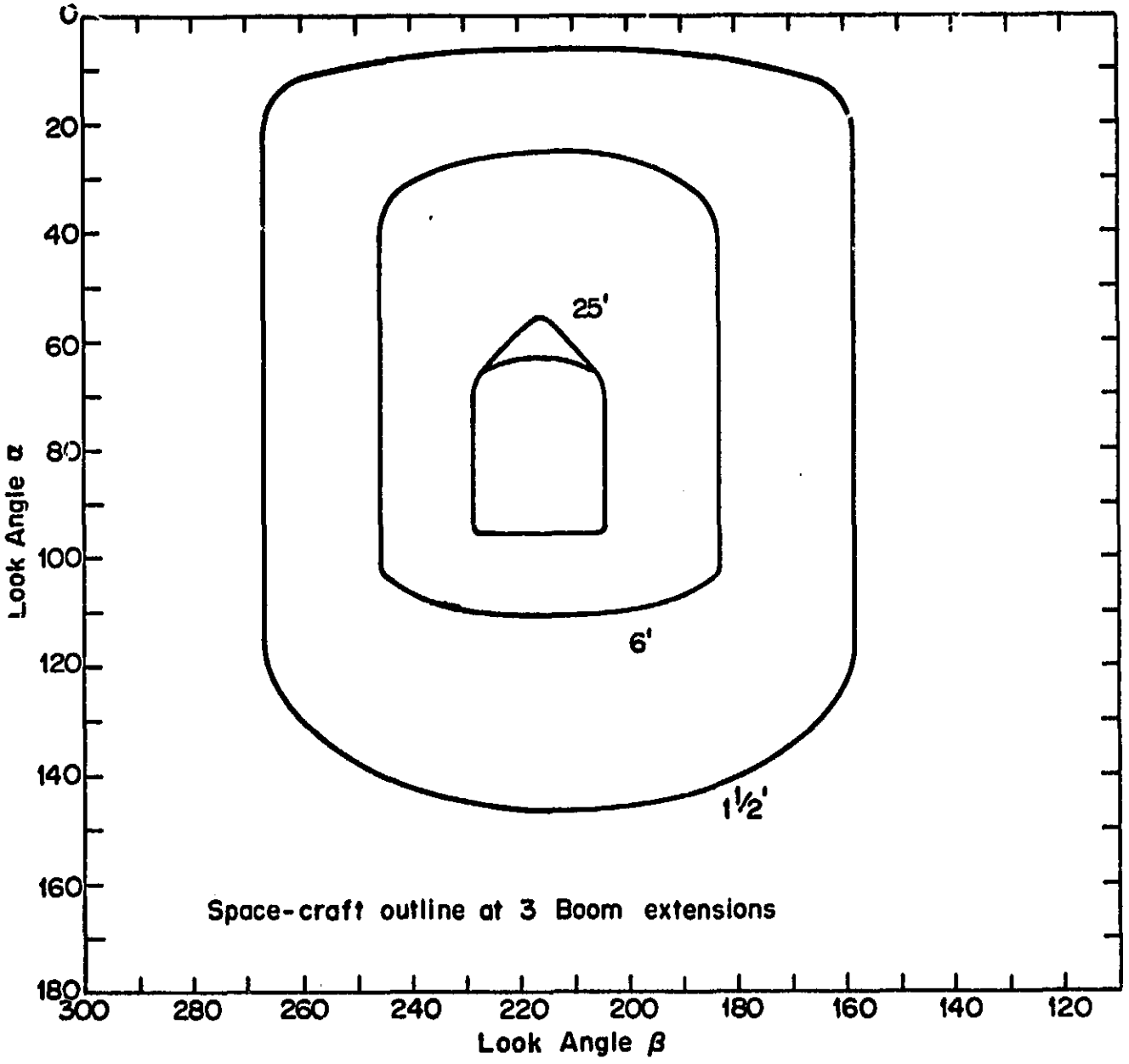
0
20
40
60
80
100
120
140
160
180
Look Angle α
300
280
260
240
220
200
180
160
140
120
Look Angle β
25'
6'
1½'
Space-craft outline at 3 Boom extensions

Fig. 5

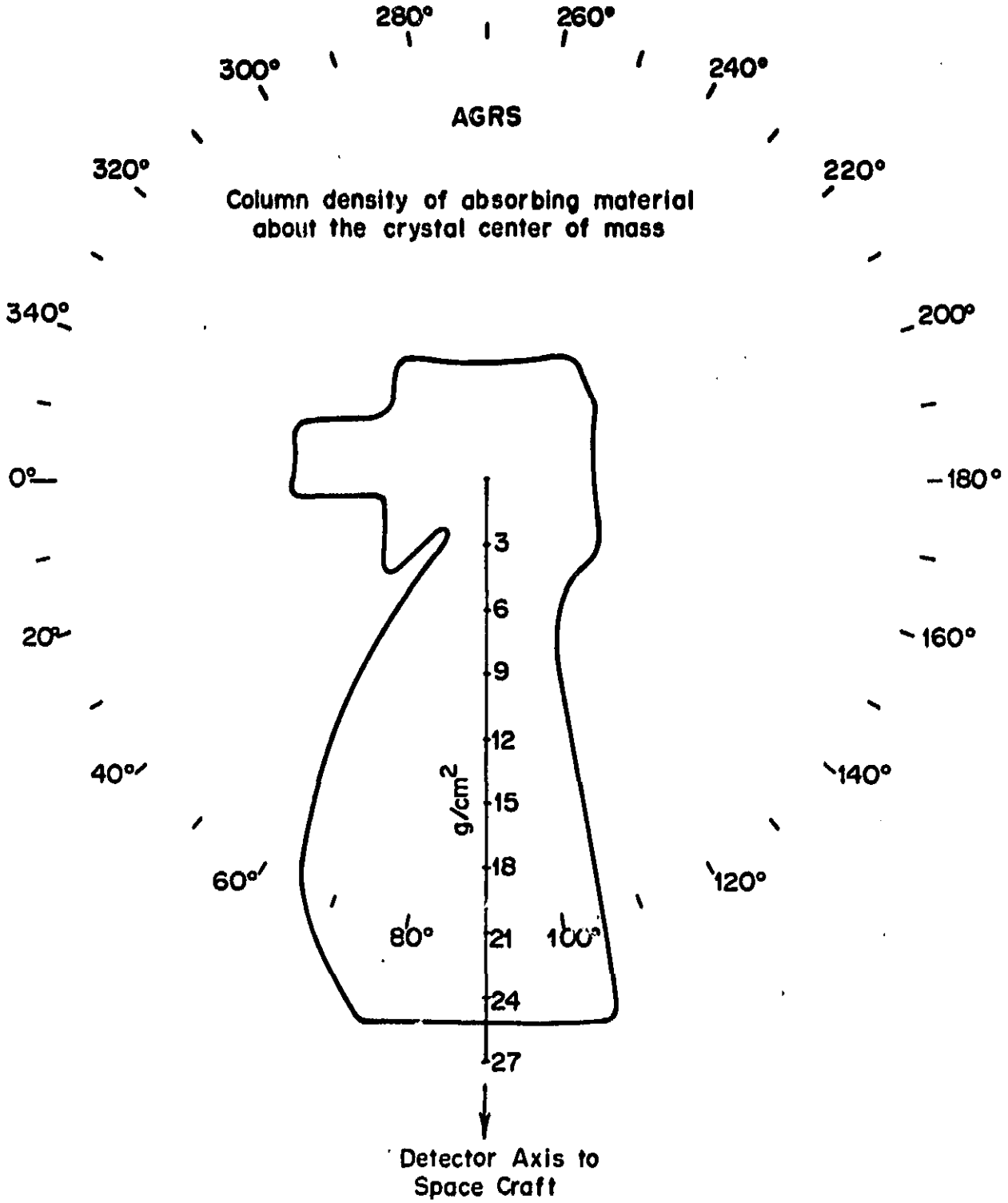
280°
260°
300°
240°
AGRS
320°
220°
Column density of absorbing material
about the crystal center of mass
340°
200°
0°
180°
20°
160°
40°
140°
60°
120°
80°
100°
3
6
9
12
15
18
21
24
27
g/cm²
Detector Axis to
Space Craft

Fig. 6

C. The Projected Area of the Detector

At the nominal position of 1.84 m (6 ft) the spacecraft occultation pattern is 62° wide and therefore one expects that the local mass will not play a significant role in the overall sensitivity function. Another factor that can be important, though, is the geometric one for a detector in the shape of a cylinder. When the detector is thick, as is the case for the AGRS, especially at a few hundred keV, the geometric sensitivity function is proportional to the projected area of the detector. For the 0.07 m x 0.07 m (7 cm x 7 cm) detector in the AGRS, the projected area is a function of the angle ζ from the axis of the cylinder:

$$A(\zeta) = \pi\left(\frac{0.07}{2}\,\mathrm{m}\right)^2 |\cos\zeta| + (0.07\mathrm{m})^2 \sin\zeta$$

$$= 3.7\cdot10^{-3}\mathrm{m}^2\,|\cos\zeta| + 4.9\cdot10^{-3}\mathrm{m}^2\sin\zeta$$

$$(= 37\ \mathrm{cm}^2\,|\cos\zeta| + 49\mathrm{cm}^2\ \sin\zeta).$$

$A(\zeta)$ has its maximum value at 53° from the axis where $A(53^{\circ}) = 6.1\cdot10^{-3}\mathrm{m}^2$ (61 cm^2) and its minimum at $\zeta = 0^{\circ}$ where $A(0^{\circ}) = 3.7\cdot10^{-3}\,\mathrm{m}^2$ (37 cm^2). The detector geometric factor, the average projected area, is $5.7\cdot10^{-3}\,\mathrm{m}^2$ (57 cm^2).

A plot of projected area vs ζ is shown in Figure 7. It is clear that this will have an effect for bright sources; the ratio of minimum to maximumprojected area is 0.61.

The local detector sensitivity function should be easy to find in the lab, and there are plans to do the tests in early 1976. Until these are completed and analyzed, the

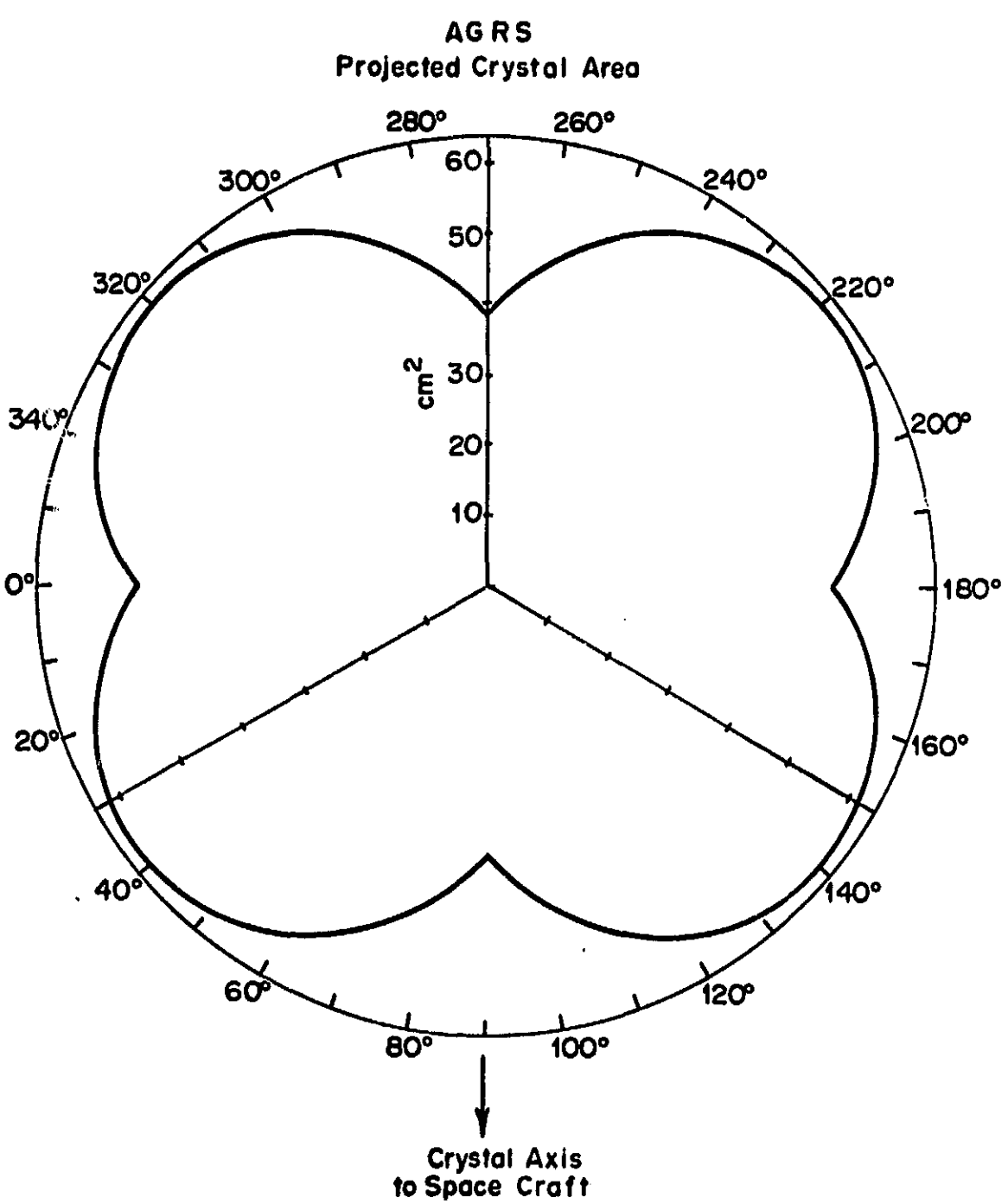
AG R S
Projected Crystal Area
280°
260°
300°
240°
60
50
320°
220°
cm²
30
340°
200°
20
10
0°
180°
20°
160°
40°
140°
60°
120°
80°
100°
Crystal Axis
to Space Craft

Fig. 7

projected area local sensitivity function is likely to be adequate for low energy gamma-ray astronomy.

D. Rate as a Function of Look Angle to the Crab

It is almost certain that the Crab is the brightest point source in the sky at ~ 150 keV during Apollo 16 TEC. The spectrum of the Crab in this energy region is well fit by the spectrum

$$\frac{dN(E)}{dE} = 3.5 \cdot 10^{-3} \left(\frac{E}{1MeV}\right)^{-2.2} \text{ photons cm}^{-2} \text{ sec}^{-1} \text{MeV}^{-1}$$

which can be integrated between 0.060 and 0.200 MeV to show that 3.6 photons sec^{-1} in this energy range are incident on the AGRS when the projected area is $5.7 \cdot 10^{-3}$ m^2 (57 cm^2). For a mean energy of 100 keV in this band, half of the photons will make it through the thermal shield and anticoincidence mantle to react with the detector. Therefore, one expects a decrease in the counting rate of ~ 1.8 counts sec^{-1} when the Crab is occulted.

Fig. 8 is an array of counting rates and their errors as a function of look angle to the Crab in the vicinity of space-craft occultation. The 6 ft, 4 ft, and 1.5 ft outlines are also drawn in. This picture suggests that the boom was out 0.46 m (1.5 ft), which is consistent with the coincidence and shield rates.

We have tried to explain the surprisingly large width by assuming the occultation pattern was really that of a 1.84 m (6 ft) boom extension and tried to solve for a second

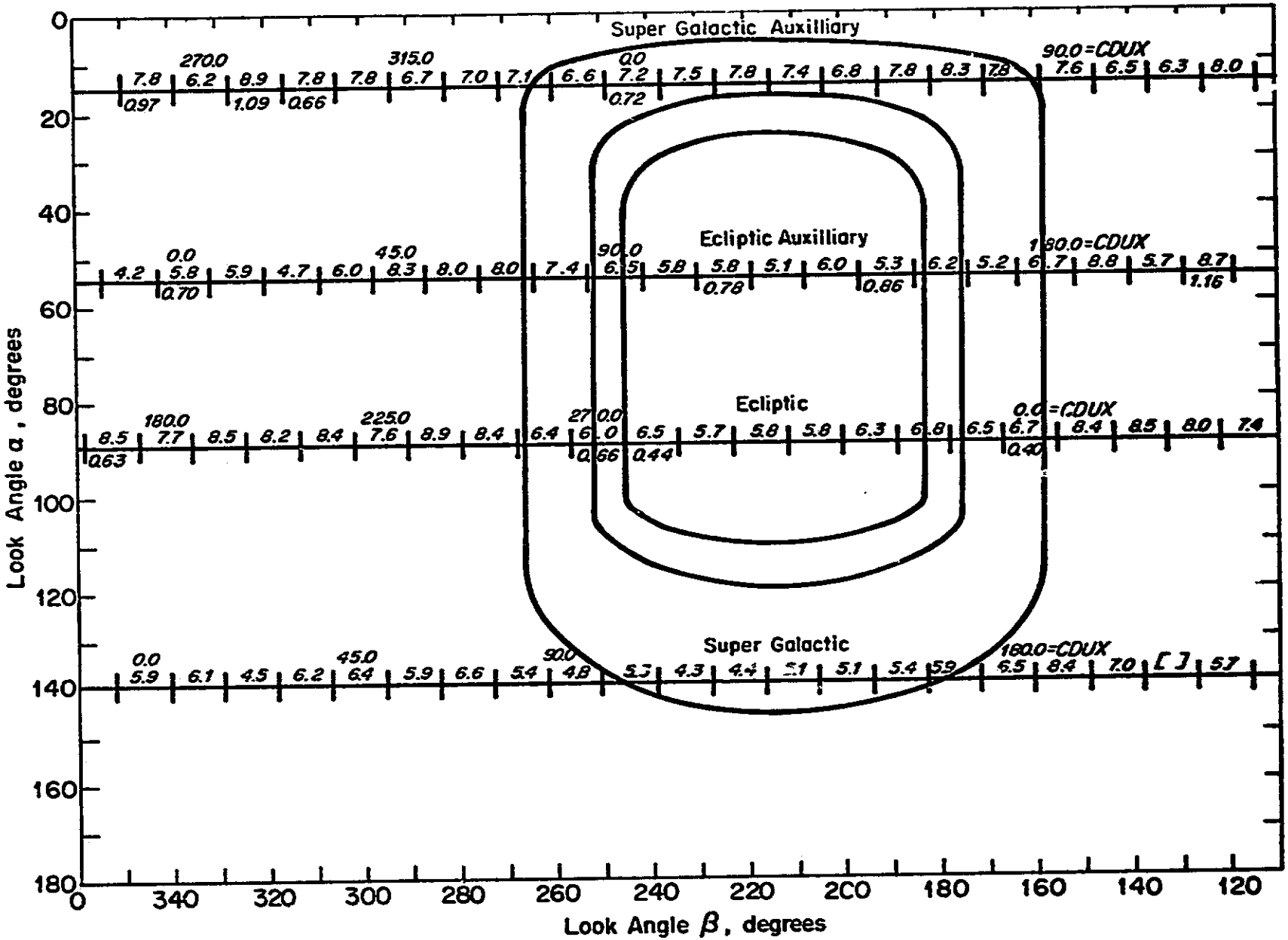

Fig. 8. Counting rate as a function of look angle to the Crab in the viscinity of space-craft occultation.

source which might account for just the width in EPTC. This procedure failed. The evidence from Fig. 8 leads one to the conclusion that the sensitivity function of the AGRS at the occultation astronomy boom position is as though the boom were deployed only 0.46 m (1.5 ft). It might be that the pattern is actually due to local mass, and if this is so, one expects to find this out in early 1976 when the local sensitivity function of the AGRS is mapped.

IV. Methods for Data Analysis

This has been the main focus of the research done at Cornell under this grant, although other areas already mentioned in this report have necessarily also been considered. The methods of analysis can be categorized by the source distribution expected to be significant in the gamma ray sky.

A. A Few Point Sources and Invariant Background

If the brightness distribution is made up simply of two or three bright point sources and an invariant background, data analysis has a particularly simple form. Any significant change in the counting rate as a function of roll angle in any PTC implies the existence of a source along some edge of the occultation pattern at that roll angle. Every decrease in the rate as a function of roll angle must then be mirrored in an increase of the same magnitude at a roll angle advanced by no more than the characteristic width of the occultation pattern. For example, if the occultation pattern is due to the space-craft and if the boom length is the nominal 1.84 m (6 ft), then the occultation of a source can be for no more than the characteristic width of the pattern, 62°. The source may be occulted for less than 62° but only if it is occulted by the top or bottom of the outline of the cylinder; in the nominal 1.84 m (6 ft) example, the limits on look angle α are $25.6^{\circ} < \alpha < 40.4^{\circ}$ (top) or $102.0^{\circ} < \alpha < 112.2^{\circ}$ (bottom).

Thus for each PTC a locus of possible source locations occurs for each significant fluctuation, and a comparison of these loci and their associated source strengths will give the point source positions. As an example, suppose that the occultation pattern is due to the spacecraft and the AGRS was only 0.46 m (1.5 ft) out on the boom. Then the decrease in rate vs. roll angle at cdux = 75°* in EAPTC implies that there is a bright source along line A in Figure 9. The decrease at cdux = 260° in EPTC implies that there is a bright source along line B. They intersect very close to the position of the Crab, and a study of the rate vs. roll angle behavior of the SGPTC and SGAPTC as other portions of the loci A and B were occulted in these modes is likely to rule out any other possible source configuration.

This procedure was carried out under the assumption of a 1.84 m (6 ft) boom position, and it was found that the decrease in rate vs. roll angle in EPTC for roll angles $270^\circ < \text{cdux} < 10^\circ$ cannot be due to any configuration of point sources. The conclusion is that the occultation pattern has a characteristic width of $\pm 55^\circ$ at least at look angles $\alpha \sim 90^\circ$ and $\alpha \sim 55^\circ$ (see Fig. 8). If the spacecraft is responsible for this occultation pattern, this implies a boom extension of 0.46 m (1.5 ft) or less.

---

*Cdux measures the amount of roll executed by the spacecraft. See the Appendix on Coordinate Systems, Section VII.

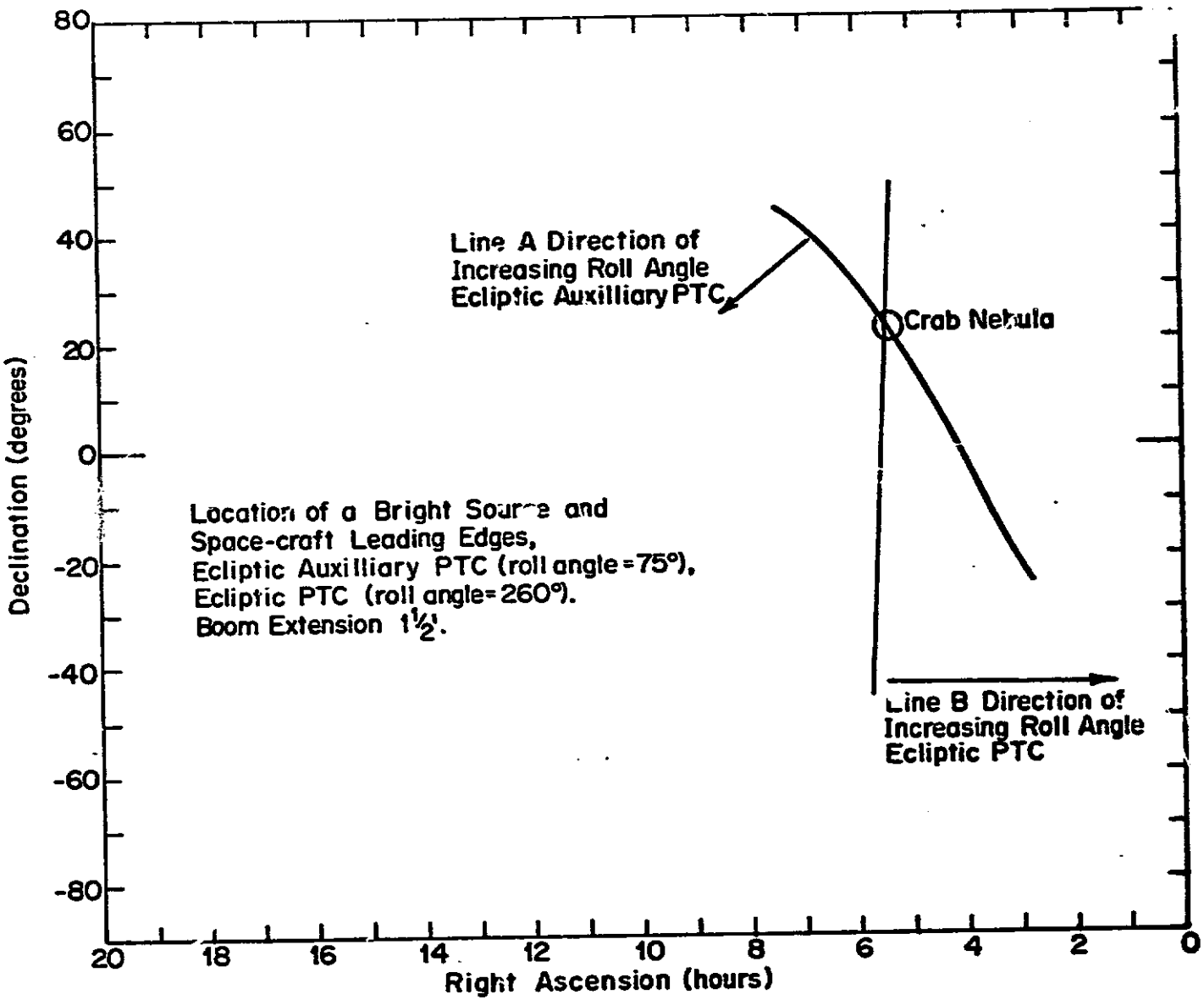
80
60
40
20
0
-20
-40
-60
-80
Declination (degrees)
20
18
16
14
12
10
8
6
4
2
0
Right Ascension (hours)
Line A Direction of Increasing Roll Angle Ecliptic Auxilliary PTC
Crab Nebula
Location of a Bright Source and Space-craft Leading Edges, Ecliptic Auxilliary PTC (roll angle=75°), Ecliptic PTC (roll angle=260°). Boom Extension 1½'.
Line B Direction of Increasing Roll Angle Ecliptic PTC

Fig. 9

B. A Few Point Sources + Line Source + Invariant Background

By a line source we mean in this report a source of gamma-rays confined to the plane of the Galaxy. One expects that it will not be a uniform distribution around the plane, and two methods for determining this distribution have been formulated.

The direct method is to divide up the Galactic plane into source regions, and accumulate counts and live-time for particular configurations of sensitivity to these source regions. To illustrate, suppose we take the 18 source regions shown in Fig. 10. Numbering the regions by i ($i = 1, 2, \ldots, I = 18$), possible point sources by k ($k = k, \ldots, K < 10$), distinct vehicle attitudes by j ($j = 1, 2, \ldots, J > I+K+1$), and letting

$f(i)$ = flux from region i in the energy interval of interest, photons $cm^{-2}sec^{-1}$,

$f(k)$ = flux from source k,

$s(i,j)$ = AGRS sensitivity to source or region i in attitude j,

R = counting rate due to the invariant background,

r_j = counting rate in attitude j,

e_j = rms error in measuring rate r_j,

one may write down an over-determined set of linear equations

$$R+\sum_{k=1}^{k} f(k)S(k,j) + \sum_{i=1}^{I} f(i)S(i,j) = r_j \pm e_j, \quad j = 1,\ldots,J.$$

These may be solved for R, the f(k) and the f(i) by the

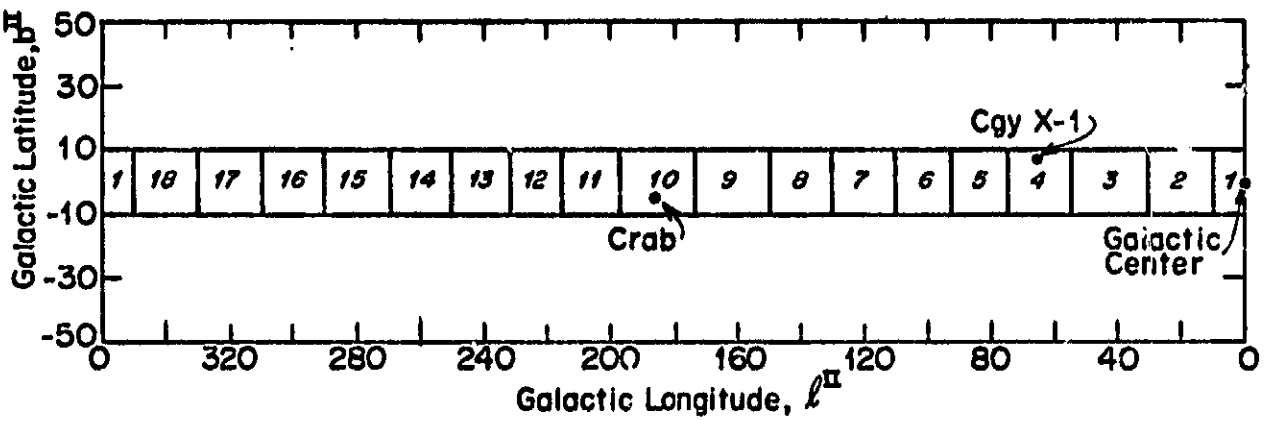

Fig. 10. 18 source regions in the Galactic plane.

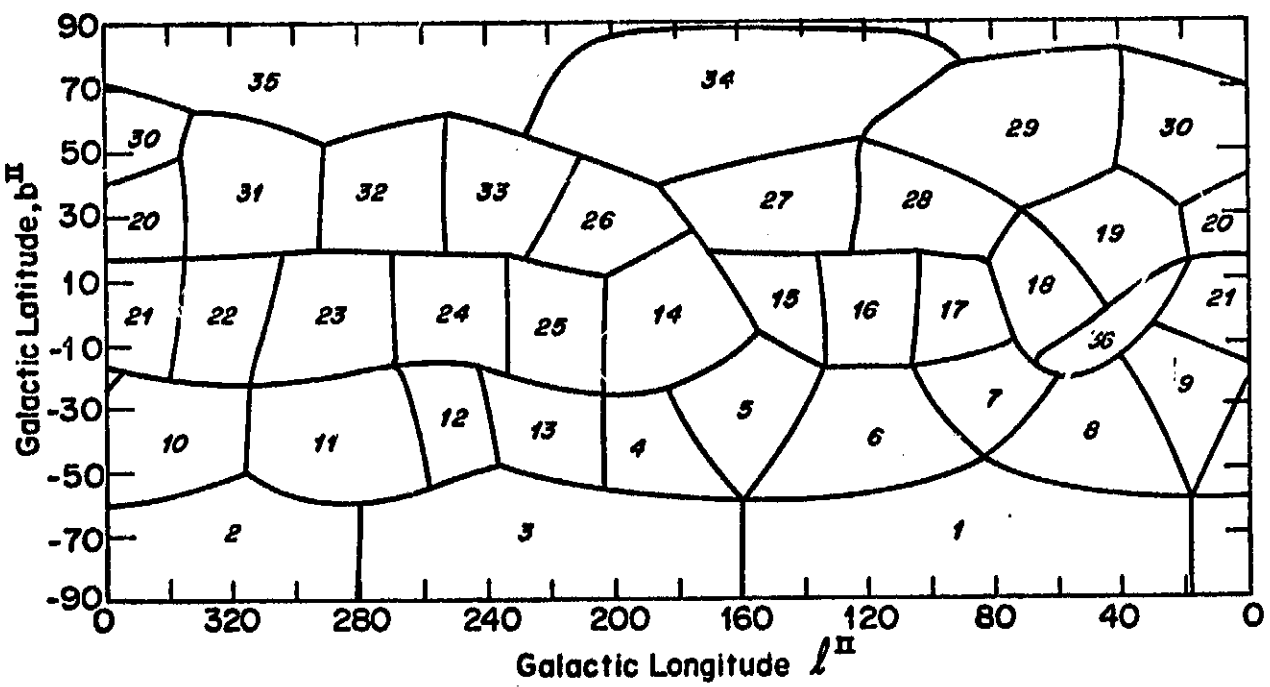

Fig. 11. 36 sky regions.

method of weighted least squares, which minimizes the χ^2 of the solution to the data. It is expected that if the brightness distribution has a measurable component which is not one of the point sources and which is not in the Galactic plane, χ^2 for the solution will be poor. Likewise if the sensitivity function depends strongly on the boom position, and the wrong boom position is assumed, χ^2 for the solution will also be poor.

The second method of analysis is the Fourier method, although one will see that the method does not use strict Fourier analysis. Consider the Galactic plane brightness distribution function after one has subtracted away the bright point sources. If this distribution is very nearly uniform, or if it is dominated by the first few Fourier components, the coefficients of these components will be significant in their own right. It is clear that under these conditions the coefficients can be more reliably determined from the data itself than from the solution by the direct method.

Assuming that the residual Galactic plane brightness distribution (bright point sources removed) has no Fourier components above some cutoff I, let

$\tilde{f}(i)$ = (complex) coefficient of the i^{th} Fourier component of the residual Galactic plane brightness distribution,

$\tilde{s}(j,j)$ = (complex) coefficient of the i^{th} Fourier component of the AGRS sensitivity function in the Galactic plane in attitude j.

Then one sees that the over-determined system of equations

$$R + \sum_{k=1}^{K} f(k)s(k,j) + \sum_{i=1}^{I} \tilde{f}(i)\tilde{s}(i,j) = r_j \pm e_j,$$

$$j = 1,\ldots,J > I=K=1.$$

can be solved, again by the method of weighted least squares yielding R, f(k), (k=1,...,K), and $\tilde{f}(i)$ (i = 1,...,I) which minimize χ^2. Again, if the assumed cutoff I is too low, if there is a measurable anisotropy in the diffuse component, or if the sensitivity function is incorrect, χ^2 is likely to be bad.

Programming the Fourier approach would not be any more difficult than programming the direct method, but one does have to worry about the uncertainty introduced by having subtracted point sources that are in the Galactic plane. One should consider these as δ functions on the Galactic plane distribution and note what an uncertainty in the brightness of the Crab, say, does to the first few Fourier components of the Galactic plane. The reason for keeping track of the rate from Crab separately is that high frequency components are present in the sensitivity function which are important for the point sources but not for the assumed residual Galactic plane distribution.

C. Anisotropic Diffuse Component

Assuming that the major extragalactic gamma ray sources, if there are any, are entered as point sources, the only other term to be fit in the brightness distribution of the

sky is anisotropy in the diffuse component. The isotropic part of the diffuse component is a term in the invariant background.

The analysis of the Apollo 16 occultation astronomy data should start with a direct approach, similar to that taken in Section B above. A choice of areas in the sky has been made to emphasize the Galactic plane and the way occultation occurred, see Fig. 11. If the areas are labelled by i, then the system of equations

$$R + \sum_{k=1}^{K} f(k)s(k,j) + \sum_{i=1}^{I} f(i)s(i,j) = r_j \pm e_j, \quad j=1,\ldots,J.$$

By putting the likely point sources in the middle of their area, one can treat them as each having an area, ascribing to the point source any excess over neighboring areas.

$$R + \sum_{i=1}^{I} f(i)s(i,j) = r_j \pm e_j, \quad j=1,\ldots,J.$$

At low energy ($\sim$ 150 keV) one expects approximately 8 areas to be occulted at one time since in any case the occultation pattern has been found to be 110° wide and must have a solid angle on the order of 3 steradians. Once the sensitivity function is known a natural definition of distinct attitude will be available; two attitudes will be said to be distinct if they occult a different combination of areas.

Since the diffuse component is known to be very uniform, it makes sense to ask about the coefficients of the anisotropy expanded in spherical harmonics. The Compton-Getting effect transforms an isotropic distribution into a

sum of an $\ell = 0$ component (isotropic) and a very small $\ell = 1$ component ($\propto \cos\theta$ from the direction of travel). This is related to the 12 and 24 hour anisotropy often sought for in such nearly isotropic distributions as the microwave background and high energy cosmic rays. For any real distribution which is expressed as a linear combination of $\ell = 0$ and $\ell = 1$ terms, an axis can be found such that the function is the sum of an isotropic component and a component $\propto \cos\theta$ from that axis. Thus one may search for the 12 and 24 hour anisotropy of the diffuse component by solving equations of the form

$$R + \sum_{k=1}^{K} f(k),s(k,j) + \sum_{i=1}^{I} f(i)s(i,j) + \sum_{m=-1}^{1} \tilde{b}_{1m}\,\tilde{s}^{*}_{im}(j) =$$

$$= r_j \pm e_j, \quad j=1,2,\ldots,J > K + I + 4$$

where the sum indexed by k is over point sources, the sum indexed by i is over the areas in the Galactic plane, and finally $s_{1m}(j)$ is the coefficient of the 1,m component of the sensitivity function in attitude j, a complex number. The b_{im} are then the coefficients of the best fit 12 + 24 hour anisotropy of the diffuse component.

Higher order spherical harmonics may be added to the equation, giving one in principle a beam solid angle of $4\pi/\ell^2$. The interference from point sources and a line source to the determination of the coefficients of anisotropy are easily computed, and generally it is clear that this procedure determines these coefficients with greater sensitivity

than one would achieve by fitting a $\cos\theta$ dependence to the results of the direct method. Again, the reason for including the point and line sources separately is that they have a considerable amount of power in high ℓ values as does the sensitivity function.

V. An Analog Model-Testing Procedure

As part of the work done under the grant, a method of testing brightness models by hand with a given sensitivity function was developed. Figure 12 shows the sensitivity function of the system to 100 keV X-rays assuming a boom extent of 0.46 m (1.5 ft) and a projected area sensitivity function under 60 kg m^{-2} (6 g cm^{-2}) of absorbing material. This is similar to a Mercator projection, and it has the nice property that a rotation about the space-craft spin axis is expressed as a simple translation of the sensitivity function. Figures 13-16 show the Galactic plane in look angle coordinates for the zero roll attitude of each PTC. The sensitivity to each part of the sky in an arbitrary roll angle during a particular PTC can be found by overlaying a transparency of Fig. 12 over the appropriate PTC figure, and translating the transparency until the fiducial marked CDUX lies over the desired roll angle. The roll angle axis is the same as the look angle β axis at zero roll.

The count rate predicted by the source model can be computed for any roll angle in any PTC in minutes, and comparing these with the observed rates allows one to calculate χ^2 for the model in a few hours. The real usefulness of the procedure, however, is that it allows one to quickly assess the merits of a particular model.

Graphs like Figures 13-16 can also be made for the pointing periods, and graphs like Figure 12 can be made for any assumed sensitivity function. The method is quite general and useful.

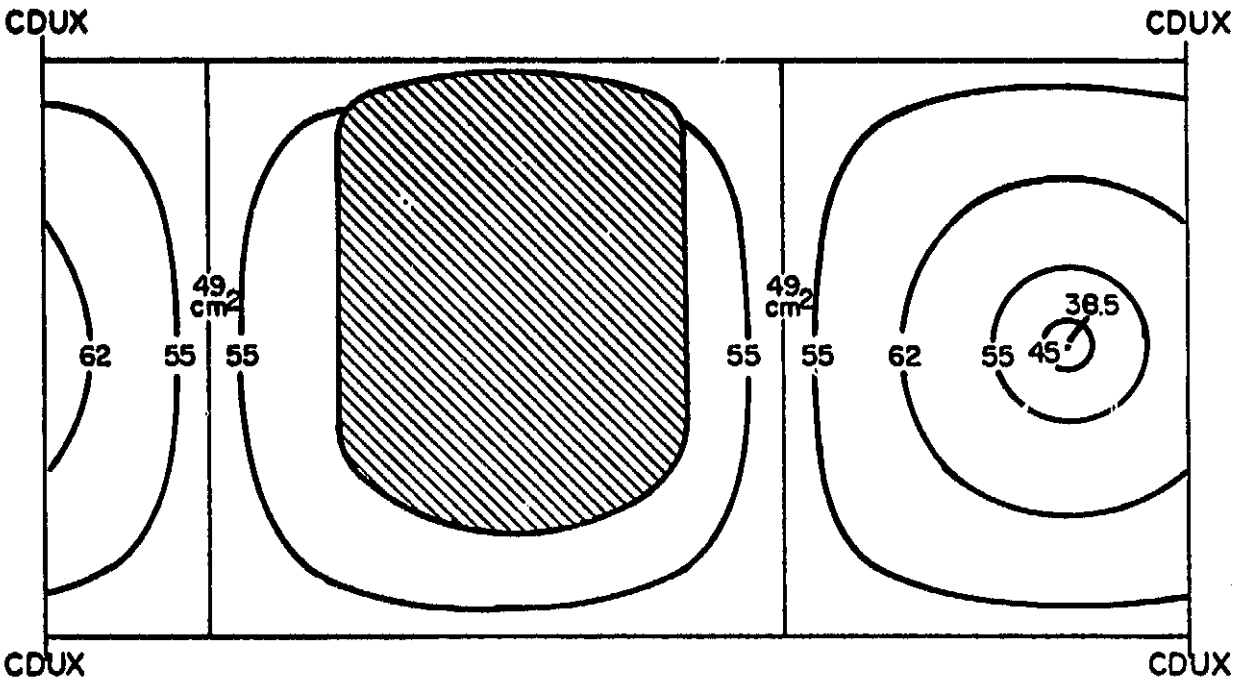

Fig. 12. Sensitivity function in look angle coordinate for 0.46m (1.5 ft) boom extension showing contours of equal projected area.

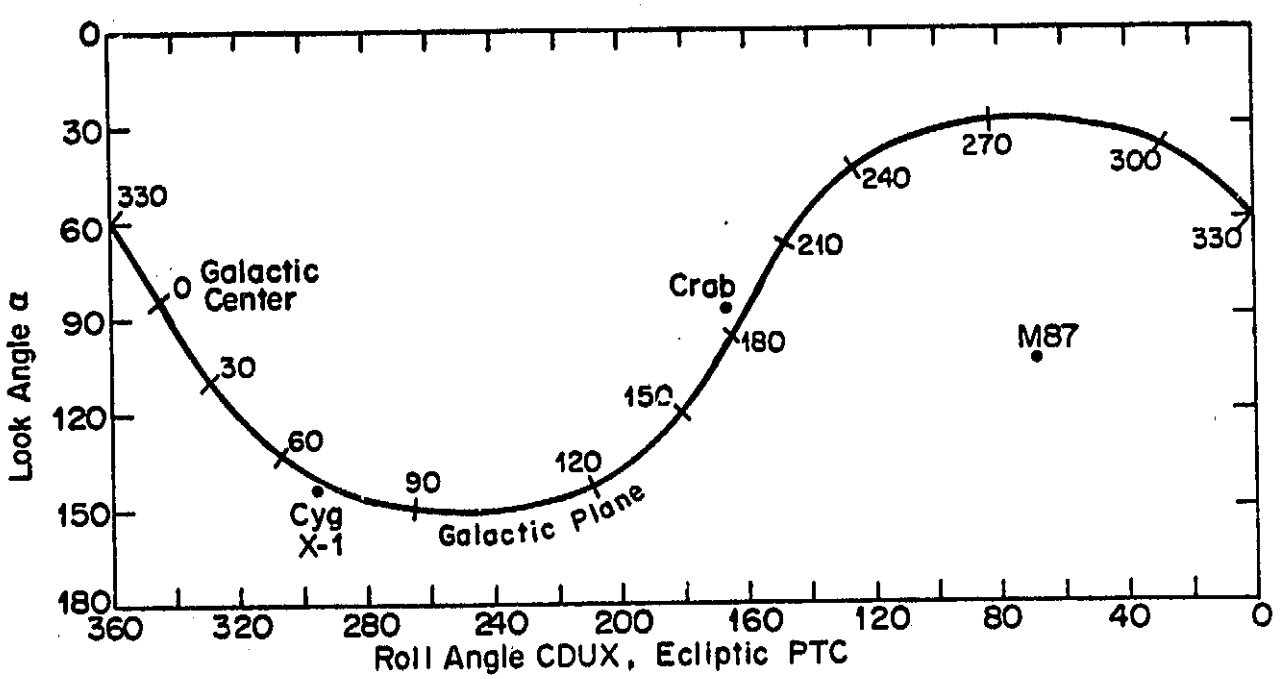

Fig. 13

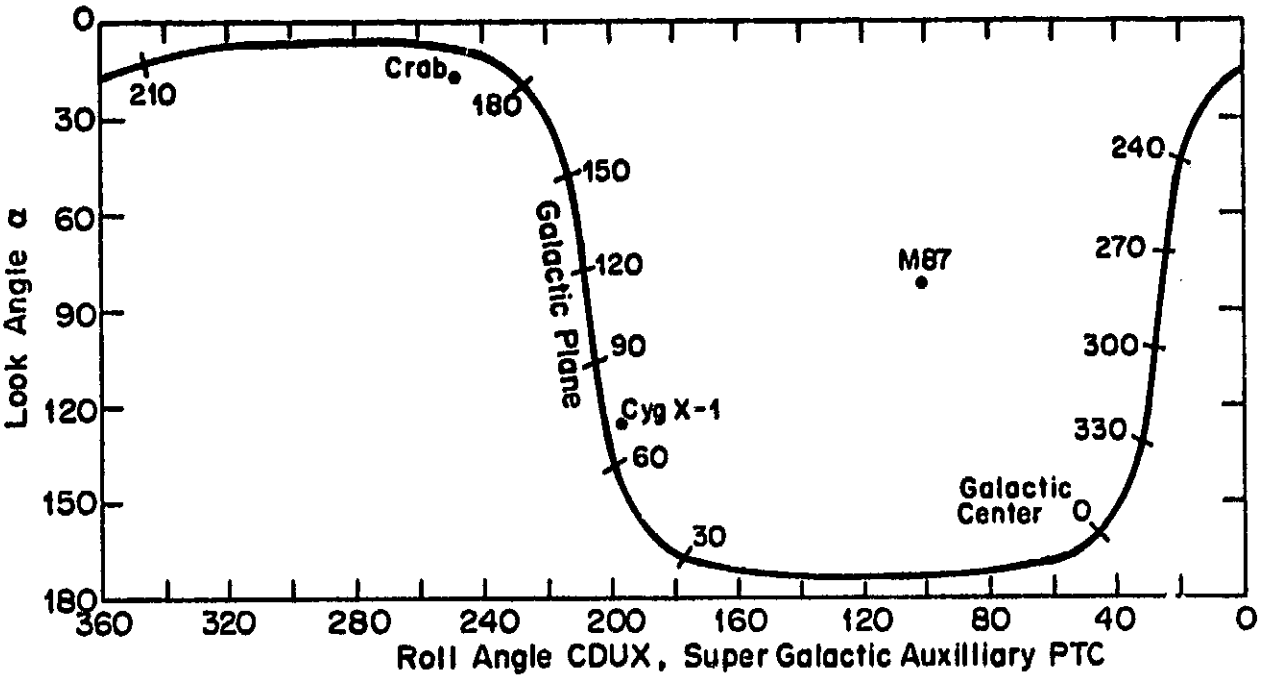
Look Angle α
0
30
60
90
120
150
180
Crab
210
180
150
120
90
60
30
Galactic Plane
Cyg X-1
M87
240
270
300
330
Galactic Center
0
360
320
280
240
200
160
120
80
40
0
Roll Angle CDUX, Super Galactic Auxilliary PTC

Fig. 14

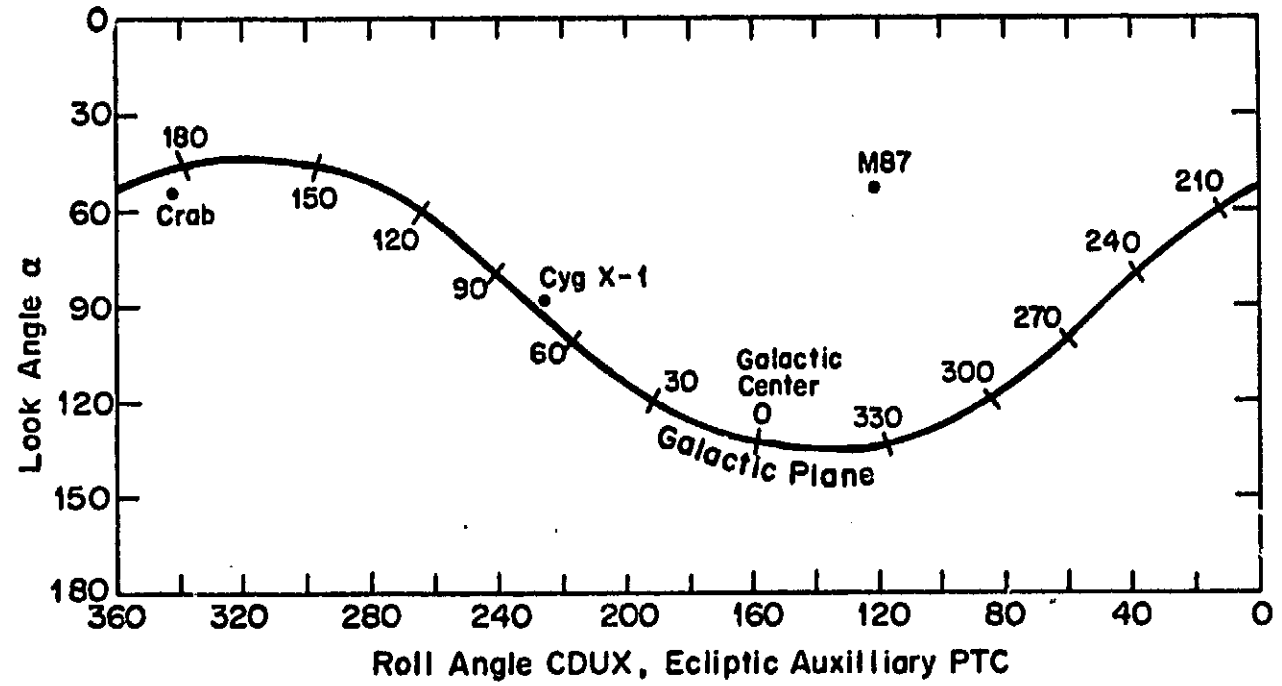
Look Angle α
0
30
60
90
120
150
180
180
Crab
150
120
90
60
30
Galactic Center
0
330
300
270
240
210
M87
Cyg X-1
Galactic Plane
360
320
280
240
200
160
120
80
40
0
Roll Angle CDUX, Ecliptic Auxilliary PTC

Fig. 15

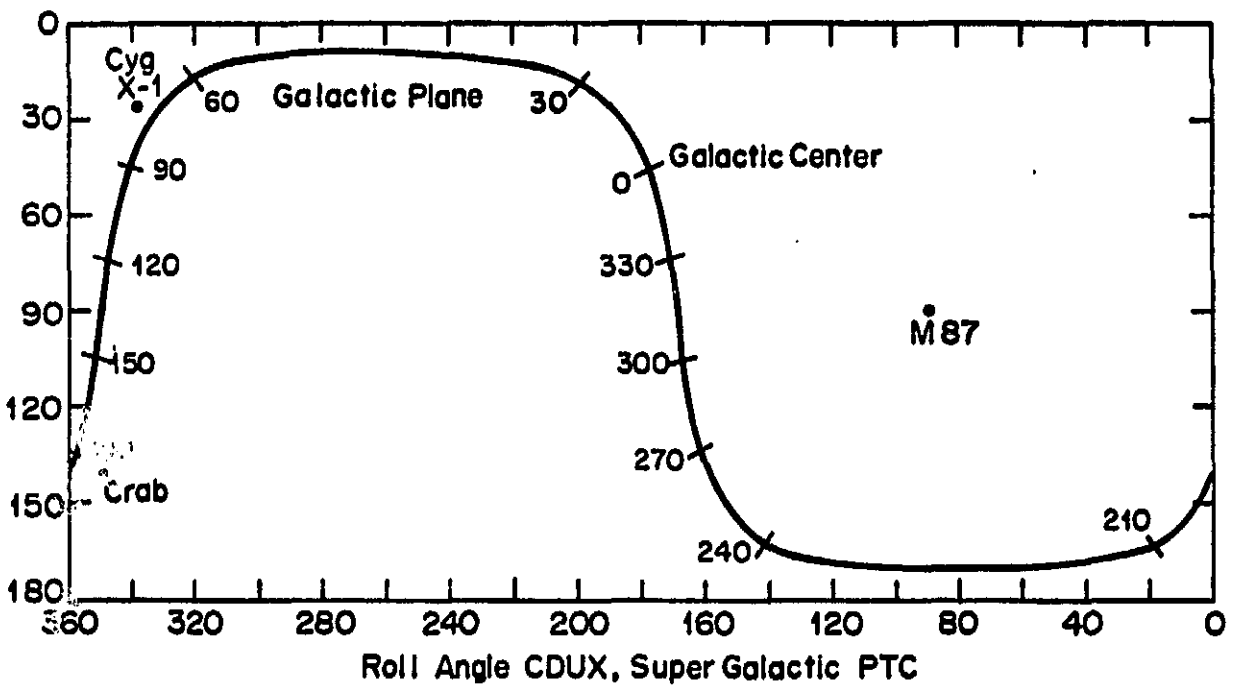
0
30
60
90
120
150
180
Cyg X-1
60
Galactic Plane
30
90
120
150
Crab
0
Galactic Center
330
300
270
240
M87
210
360
320
280
240
200
160
120
80
40
0
Roll Angle CDUX, Super Galactic PTC

Fig. 16

VI. Conclusions

There are two primary conclusions to the work mentioned in this report. First, the Crab nebula and a source near the Galactic center are clearly visible in the Apollo 16 occultation astronomy data, and evidently much other astronomical information is there also. Second, the sensitivity function of the detector during the occultation astronomy portion of TEC is not satisfactorily known. The detector count rates and the timing of boom extensions and retractions imply the detector was the nominal 1.84 m (6 ft) from the space-craft while the occultation pattern of the Crab and the coincidence counting rates lead one to think the detector was 0.46 m (1.5 ft) out on its boom.

However, given the correct sensitivity function one expects interesting astronomical results in this important energy region.

VII. Appendix on Coordinate Systems

A. Three Inertial Coordinate Systems

Directions in the sky are usually identified as points on a sphere with two reference points given, a pole and a point on the equator. A latitude is measured relative to the point on the pole and a longitude relative to the point on the equator, and when these reference points are fixed relative to the distant stars, they are said to be inertial.

Three inertial coordinate systems are useful in gamma-ray astronomy from the Apollo space vehicle. The first is the familiar equatorial coordinate system which has the spin axis of the earth as a pole and the direction from the earth to the sun at the vernal equinox (defined to lie on the equator of the earth) as the reference point on the equator. Due to a slow wobble of the earth on its axis, this coordinate system is not quite inertial, but in this report the coordinate system of 1950.0 is the same as that of 1972.0. The coordinates of the equatorial system are the longitude A called right ascension and measured in hours ($1^{hr} = 15^{o}$ on the equator) and the declination D which is 0^{o} on the equator and $+90^{o}$ at the north pole.

The second useful coordinate system is called the second Galactic coordinate system. The pole is taken as the north pole of the plane of our Galaxy, and the zero of Galactic longitude is the Galactic center. Galactic longitude is denoted ℓ in this report and is measured in degrees

as is Galactic latitude b, defined so that $+90^{\circ}$ is the north Galactic pole.

The third system was adapted for the convenience of the Apollo 16 mission and uses the ecliptic plane as its equator. The attitude of the vehicle was measured relative to this inertial system by the Inertial Measurement Unit, giving the coordinates their name, the IMU system. This system is defined in terms of the equatorial system, and does not usually have a lattitude and longitude associated with it.

Another way of specifying a direction in the sky is to give the three components of the unit vector having that direction. Again, this requires the definition of two reference directions, which become axes x and z, the directions of longitude reference and lattitude reference, respectively. Axis y is defined by the cross-product $y = z \cdot x$ to give a right handed system. For the equatorial system

$$\begin{pmatrix} x \\ y \\ z \end{pmatrix}_{eq} = \begin{pmatrix} \cos(A)\cos(D) \\ \sin(A)\cos(D) \\ \sin(D) \end{pmatrix}$$

while for the Galactic system

$$\begin{pmatrix} x \\ y \\ z \end{pmatrix}_{Gal} = \begin{pmatrix} \cos(\ell)\cos(b) \\ \sin(\ell)\cos(b) \\ \sin(b) \end{pmatrix}$$

The relation between two coordinate systems may then be given by a matrix M which has the property that its inverse is simply its transpose, $M^{-1} = M^{T}$.

To give a specific useful example, the matrix G in the equation

$$\begin{pmatrix} x \\ y \\ z \end{pmatrix}_{Gal} = G \begin{pmatrix} x \\ y \\ z \end{pmatrix}_{eq}$$

is given by

$$G = \begin{bmatrix} -.067031, & -.872717, & -.483602 \\ 0.492723, & -.450521, & 0.744543 \\ -.867601, & -.188375, & 0.460200 \end{bmatrix}$$

The inverse equation is

$$\begin{pmatrix} \cos(A)\cos(D) \\ \sin(A)\cos(D) \\ \sin(D) \end{pmatrix} = \begin{bmatrix} -.067031, & 0.492723, & -.867501 \\ -.872717, & -.450421, & -.188375 \\ -.483602, & 0.744543, & 0.460200 \end{bmatrix} \begin{pmatrix} \cos(\ell)\cos(b) \\ \sin(\ell)\cos(b) \\ \sin(b) \end{pmatrix}$$

Finally, the matrix R giving IMU system in terms of the equatorial system,

$$\begin{pmatrix} x \\ y \\ z \end{pmatrix}_{IMU} = R \begin{pmatrix} x \\ y \\ z \end{pmatrix}_{eq} ,$$

is called the REFSMMAT for REFerence Stable Member MATrix. It is changed during different phases of the mission but during the time that the basic AGRS astronomy data base was acquired

$$R = \begin{bmatrix} -.342020, & -.862128, & -.373841 \\ -.939693, & 0.313789, & 0.136067 \\ 0.0, & 0.397833, & -.917458 \end{bmatrix}$$

B. Space Vehicle Coordinate Systems

Since the Apollo Command and Service Module (CSM) is basically a figure of revolution, its x axis is chosen to be the axis of symmetry, and is called the roll axis. The z, or yaw, axis is defined by a bench-mark on the CSM to be in the direction of the seated astronaut's head. Making a right-handed system the y, or pitch axis, is defined by the cross product

$$y = z \wedge x \quad .$$

The direction to celestial objects in terms of the instantaneous vehicle axes gives another coordinate system in the sky which is a function of the attitude of the vehicle. The latitude and longitude coordinates of the space-craft are called look angles α and β respectively, but they are defined in a peculiar way for the convenience of the astronauts. The look angle α of a celestial object is defined as the angle between the vehicle roll axis (+x) and the object, and one sees that objects in the direction of the roll axis have $\alpha = 0^{\circ}$ while objects in the vehicle equator have $\alpha = 90^{\circ}$. Look angle β measure longitude from the vehicle -z axis which is in the direction of the seated astronaut's feet. The center of view for instruments in the Scientific Instrument Module (SIM) was $\alpha = 90^{\circ}$, $\beta = 37.75^{\circ}$. In general, the unit vector in vehicle coordinates of a given line of sight is related to the look angles by

$$\begin{pmatrix} x \\ y \\ z \end{pmatrix}_{veh} = \begin{pmatrix} \cos(\alpha) \\ \sin(\beta)\sin(\alpha) \\ -\cos(\beta)\sin(\alpha) \end{pmatrix}$$

The attitude of the space-craft is expressed as if it were performed in the sequence of pitch, yaw, and roll. The gimbal angles of the gyros in the inertial measurement unit are telemetered from the Control Display Unit (CDU) and are identified as CDUX, the roll angle, CDUY, the pitch angle, and CDUZ, the yaw angle. When CDUX = CDUY = CDUZ = 0, the vehicle axes define the Cartesian axes of the IMU system, and one may relate look angles to equatorial coordinates by the transpose of the matrix R.

$$\begin{pmatrix} x \\ y \\ z \end{pmatrix}_{eq} = R^T \begin{pmatrix} x \\ y \\ z \end{pmatrix}_{IMU}$$

In an arbitrary attitude

$$\begin{pmatrix} x \\ y \\ z \end{pmatrix}_{veh} = [CDUX]\cdot[CDUZ]\cdot[CDUY] \begin{pmatrix} x \\ y \\ z \end{pmatrix}_{IMU}$$

where the matrices

$$[CDUX] = \begin{bmatrix} 1 & 0 & 0 \\ 0 & \cos(CDUX) & \sin(CDUX) \\ 0 & -\sin(CDUX) & \cos(CDUX) \end{bmatrix}$$

$$[CDUZ] = \begin{bmatrix} \cos(CDUZ) & \sin(CDUZ) & 0 \\ -\sin(CDUZ) & \cos(CDUZ) & 0 \\ 0 & 0 & 1 \end{bmatrix}, \text{ and}$$

$$[CDUY] = \begin{bmatrix} \cos(CDUY) & 0 & -\sin(CDUY) \\ 0 & 1 & 0 \\ \sin(CDUY) & 0 & \cos(CDUY) \end{bmatrix} .$$

Calling the product matrix M = M(CDUX,CDUY,CDUZ)

$$M = [CDUX] \cdot [CDUZ] \cdot [CDUY] ,$$

one relates vehicle and equatorial by

$$\begin{pmatrix} x \\ y \\ z \end{pmatrix}_{veh} = MR \begin{pmatrix} x \\ y \\ z \end{pmatrix}_{ea} , \text{ and}$$

$$\begin{pmatrix} x \\ y \\ z \end{pmatrix}_{eq} = R^T M^T \begin{pmatrix} x \\ y \\ z \end{pmatrix}_{veh} .$$

In specifying the look angles to a celestial object, the origin of the vehicle coordinate system need not be given, but f r a discussion of points in and near the space-craft, the origin is taken to be on the roll axis 25.6 m (1000 inches) below the bottom of the heat shield.

REFERENCES

1. Arnold, J.R., Metzger, A.E., Peterson, L.E., Reedy, R.D., Trombka, J.E., Apollo 16 Preliminary Science Report, NASA SP-315, 18-1 (1972).

2. Harrington, T.M., Marshall, J.H., Arnold, J.R., Peterson, L.E., Trombka, J.I., Metzger, A.E., Nucl. Inst. Meth., 118, 401 (1974).

3. Metzger, A.E., Parker, R.H., Gilman, D., Peterson. L.E., Trombka, J.I., Ap.J. (Letters), 194, L19 (1974).

4. Trombka, J.I., Metzger, A.E., Arnold, J.R., Matteson, J.L., Reedy, R.C., Peterson, L.E., Ap.J., 181, 737 (1973).

5. Trombka, J.E., Schmadebeck, R.L., Eller, E.L., Adler, I., Metzger, A.E., Gilman, D., Gorenstein, P., Bjorkholm, P., Ap.J. (Letters), 194, L27 (1974).

6. Trombka, J.I., Vette, J.I., Stecker, F.W., Eller, E.L., Wildes, W.T., Nucl. Inst. Meth., 117, 99 (1974), Nucl. Inst. Meth., 1.

7. Wolfe, A.M., Ap.J. (Letters), 159, L61 (1970).